Molecular Physics, Vol. 103, No. 6–8, 20 March–20 April 2005, 1027–1034

Taylor & Francis
Taylor & Francis Group

Effects of large-amplitude torsions on partition functions: beyond the conventional separability assumption

B.M. WONG and W.H. GREEN Jr*
Massachusetts Institute of Technology, MA, USA

(*Received 12 August 2004; accepted 29 October 2004*)

Large-amplitude motions, particularly internal rotations, significantly affect thermochemical properties and reaction rates. The conventional method for computing partition functions, developed by Pitzer more than 50 years ago, is based on the assumption of large-amplitude motion being completely separable from other vibrational degrees of freedom. However, no convenient method is available to assess the accuracy of Pitzer's approximation. A precise variational method, suitable for computing the coupling between large- and small-amplitude motions in small molecules, has previously been developed by Tew, Carter, Handy, and co-workers and applied to a few cases. Here, a method is presented for computing the effects of this coupling that is more suitable for routine computations of partition functions of large polyatomics. The couplings of all the vibrational modes to a large-amplitude torsion are analysed in the molecule *ortho*-chlorotoluene. An approach to defining the internal rotational angle along the torsional coordinate for symmetric rotors is also discussed. Finally, the error introduced by the conventional separability assumption is computed to identify which cases require a higher level treatment.

1. Introduction

The canonical partition function $Q(T)$ is the principal quantity used to connect quantum chemical calculations and spectroscopic data with crucial technological parameters: thermochemical quantities (entropies, heat capacities) and reaction rates via transition state theory. These thermochemical quantities and rates are used in a variety of computations and simulations that strongly influence governmental regulations, business decisions, and the design, hazard assessment, control, and improvement of industrial processes. As quantum chemical calculations are becoming both accurate and computationally affordable, they are becoming the method of choice for estimating reaction rates and are becoming competitive with other methods for estimating thermochemical data. It is therefore important to carefully consider how the approximations made in conventional partition function calculations affect these rate and thermodynamic estimates.

The conventional statistical–mechanical approach to computing the partition functions of polyatomic molecules and transition states involves assuming the many vibrational modes of the system are separable, i.e. it is typically assumed that

$$Q = Q_{\text{trans}} Q_{\text{rot}} \prod_i Q_i, \tag{1}$$

where Q_i is the partition function of the ith vibrational mode. Each vibrational mode is usually assumed to be a harmonic oscillator, a free internal rotor, or a hindered internal rotor. The implicit assumption of equation (1) is that there exists a separable Hamiltonian

$$\hat{H} = \hat{H}_{\text{trans}} + \hat{H}_{\text{rot}} + \sum_i \hat{H}_i, \tag{2}$$

which is an accurate enough zeroth-order approximation to the true Hamiltonian such that the Q computed using equation (1) is a close approximation to the true partition function of the system. This approach is widely used for computing reaction rates, and is carefully presented from both a classical and a quantum point of view in H.S. Johnston's classic text *Gas Phase Reaction Rate Theory* [1].

If all the modes can be described as small-amplitude motions, and particularly if the vibrational frequencies are all greater than $k_B T/h$, a normal-mode harmonic oscillator treatment is very reasonable; therefore, one would expect the Q computed using equation (1)

* Corresponding author. e-mail: whgreen@mit.edu

Molecular Physics
ISSN 0026–8976 print/ISSN 1362–3028 online © 2005
Taylor & Francis Group Ltd
http://www.tandf.co.uk/journals
DOI: 10.1080/00268970412331333627

to accurately reproduce the true Q. However, in many cases there are modes such as internal rotations, which are known to have large amplitudes even at very low energies, and it is much less clear that equation (1) should be accurate. When there is a large-amplitude motion, such as an internal rotor coordinate s, the Hamiltonian cannot be separable to quadratic order unless both the potential and kinetic energy couplings are negligible for all values of s. In addition, one frequently finds that equilibrium bond lengths and angles are functions of s. In many cases there will be more than one large-amplitude rotor mode, and these will all be coupled together as well as to all the normal modes. In the present paper we focus on the case where there is only one large-amplitude rotor significantly coupled to the other modes.

If all these coupling effects are indeed negligible, Pitzer and Gwinn [2, 3] developed reliable and widely used methods for estimating the partition function for the internal rotor mode. There has been some progress on this problem in the six decades since Pitzer and Gwinn's paper, but the modern literature is not clear on the criteria for determining whether these s-dependent couplings are negligible from the point of view of computing a partition function. Certainly these couplings can cause very serious perturbations in the energy levels, as is frequently observed in high resolution spectroscopy [4]. Fortunately, most of these complicated details are averaged out when computing a thermal partition function. All the available evidence suggests the separability approximation is quite successful for computing the thermodynamic properties of most stable molecules, and indeed many of the entropy and heat capacity numbers found in the standard data tables [5] are calculated assuming separability and the Pitzer–Gwinn approximation. Here, we directly test the separability approximation by computing the partition functions including all the first-order couplings between the small-amplitude vibrations and the large-amplitude rotor. We investigate these couplings within the framework of an internal coordinate path Hamiltonian developed by Tew, Handy, and co-workers [6]. This Hamiltonian characterizes large-amplitude motion in terms of an internal coordinate path which lies close to the minimum energy path. The internal coordinate path of course depends on the different possible definitions for the internal rotation angular coordinate s, since differences in the definition of s can sometimes lead to large changes in molecular parameter values. Here we present calculations on *ortho*-chlorotoluene to put this discussion on a quantitative basis. The conditions where the couplings of torsions to vibrations is likely to materially affect the partition function and reaction rate are laid out.

2. Hamiltonian

The theory of the internal coordinate path Hamiltonian is expressed in terms of a single large-amplitude coordinate s, its conjugate momentum p_s $(= -i\hbar\,\partial/\partial s)$ and the coordinates Q_k $(k = 1, 2, \ldots, 3N\text{–}7)$ and momenta P_k $(= -i\hbar\,\partial/\partial Q_k)$ of the orthogonal small-amplitude vibrational modes. A detailed method for solving this Hamiltonian using a variational method is described by Tew *et al.* [6]. We begin with the quantum mechanical kinetic energy operator

$$\hat{T} = \frac{1}{2}\sum_{d,e=1}^{4} \mu^{1/4}\left(\hat{\Pi}_d - \hat{\pi}_d\right)\mu_{de}\mu^{-(1/2)}\left(\hat{\Pi}_e - \hat{\pi}_e\right)\mu^{1/4} + \frac{1}{2}\sum_k \mu^{1/4}\hat{P}_k\mu^{-(1/2)}\hat{P}_k\mu^{1/4}. \tag{3}$$

Π and π are four-component operators

$$\begin{aligned} \hat{\Pi} &= \left(\hat{J}_x, \hat{J}_y, \hat{J}_z, \hat{p}_s\right) \\ \hat{\pi} &= \sum_{kl}\left(B_{kl,x}(s), B_{kl,y}(s), B_{kl,z}(s), B_{kl,s}(s)\right)Q_k\hat{P}_l \end{aligned} \tag{4}$$

where J_x, J_y, and J_z are the components of the total angular momentum operator, and B_{kl} is the Coriolis coupling, defined as

$$\begin{aligned} B_{kl,\alpha}(s) &= \sum_i\sum_{\beta\gamma}\varepsilon_{\alpha\beta\gamma}L_{i\beta,k}(s)L_{i\gamma,l}(s) \\ B_{kl,s}(s) &= \sum_i\sum_{\alpha}L'_{i\alpha,k}(s)L_{i\alpha,l}(s). \end{aligned} \tag{5}$$

$\mathbf{L}_k(s)$ is the kth normal mode eigenvector of the Hessian matrix at s from which translations, rotations, and motion along the path have been projected. Here, i and $\alpha\beta\gamma$ denote the ith atom and the xyz Cartesian components respectively. One also requires the following definitions

$$\begin{aligned} \mu_{de}(s, \mathbf{Q}) &= \sum_{a,b=1}^{4}(\mathbf{I}_0 + \mathbf{b})^{-1}_{da}\mathbf{I}_{0ab}(\mathbf{I}_0 + \mathbf{b})^{-1}_{be} \\ \mu(s, \mathbf{Q}) &= \det(\mu_{de}). \end{aligned} \tag{6}$$

The symmetric inertia matrix $\mathbf{I}_0$ is

$$\mathbf{I}_0 = \begin{pmatrix} I_{0xx} & I_{0xy} & I_{0xz} & I_{0xs} \\ I_{0yx} & I_{0yy} & I_{0yz} & I_{0ys} \\ I_{0zx} & I_{0zy} & I_{0zz} & I_{0zs} \\ I_{0sx} & I_{0sy} & I_{0sz} & I_{0ss} \end{pmatrix}, \tag{7}$$

where $I_{0\alpha\beta}$ are the elements of the 3×3 Cartesian inertia tensor along the path. The other terms $I_{0\alpha s}$ and I_{0ss} are given by

$$\begin{aligned} I_{0\alpha s} &= I_{0s\alpha} = \sum_i \sum_{\beta\gamma} \varepsilon_{\alpha\beta\gamma} a_{i\beta} a'_{i\gamma} \\ I_{0ss} &= \sum_i \sum_\alpha a'_{i\alpha} a'_{i\alpha}. \end{aligned} \tag{8}$$

$\mathbf{a}_i(s)\,(= m_i^{1/2}\mathbf{r}_i(s))$ are the reduced mass Cartesian coordinates of the ith atom at any point on the path 's' with respect to molecule-fixed axes, and $\mathbf{a}'_i(s) = \mathrm{d}\mathbf{a}_i(s)/\mathrm{d}s$. These geometries are computed by optimizing the molecular geometry using a quantum chemistry code (in our case, Gaussian 98 [7]) while holding a selected internal coordinate θ fixed, and then rotating to the molecule-fixed Eckart frame using the method of Carter and Handy [8]. All that remains is to define $\mathbf{b}$; in the following discussion, we will see it is not necessary to know the explicit form of $\mathbf{b}$ other than it is a 4×4 matrix which is only linear in Q_k.

The exact kinetic energy operator in these coordinates is too complicated to work with directly for the dense spectra of large polyatomic molecules. Analogous to the standard treatment of perturbation theory, we can expand equation (3) in terms of the small-amplitude coordinates Q_k. This makes it possible to use various approximations to the Hamiltonian which are manageable. The effective moment of inertia matrix depends weakly and linearly on the small-amplitude coordinates Q_k. Expanding μ_{de} in the vibrational normal coordinates and retaining the first term depending only on s gives

$$\mu_{de}(s, \mathbf{Q}) = \sum_{a,b=1}^{4} (\mathbf{I}_0 + \mathbf{b})^{-1}_{da} \mathbf{I}_{0ab} (\mathbf{I}_0 + \mathbf{b})^{-1}_{be} \approx \mathbf{I}^{-1}_{0de}(s). \tag{9}$$

Substituting equation (9) into equation (3), we obtain the approximate kinetic energy operator

$$\begin{aligned} \hat{T} = {} & \frac{1}{2} \sum_{d,e=1}^{4} \mu_{de} \left(\hat{\Pi}_d - \hat{\pi}_d \right) \left(\hat{\Pi}_e - \hat{\pi}_e \right) \\ & + \frac{1}{2} \sum_{d=1}^{4} (\hat{p}_s \mu_{sd}) \left(\hat{\Pi}_d - \hat{\pi}_d \right) \\ & + \frac{1}{2} \mu^{1/4} \left[\hat{p}_s \mu_{ss} \mu^{-(1/2)} \left(\hat{p}_s \mu^{1/4} \right) \right] + \frac{1}{2} \sum_k \hat{P}_k^2, \end{aligned} \tag{10}$$

where the operator p_s operates only within the parentheses and brackets in equation (10). To remove some of the coupling terms in equation (10) we choose molecule-fixed axes by numerically enforcing the Eckart conditions

$$\sum_i \mathbf{a}_i(s) \times \mathbf{a}'_i(s) = 0. \tag{11}$$

Since the Eckart conditions are obeyed, $\mathbf{I}_{0\alpha s} = \mathbf{I}_{0s\alpha} = 0$, and therefore $\mu_{\alpha s} = \mu_{s\alpha} = 0$. It follows from equations (10) and (11) that the kinetic energy operator for total angular momentum $J = 0$ can be written in the following form:

$$\begin{aligned} \hat{T} = {} & \frac{1}{2} \sum_{d,e=1}^{3} \mu_{de} \hat{\pi}_d \hat{\pi}_e + \frac{1}{2} \mu_{ss} \left(\hat{p}_s^2 - \hat{p}_s \hat{\pi}_s - \hat{\pi}_s \hat{p}_s + \hat{\pi}_s^2 \right) \\ & + \frac{1}{2} (\hat{p}_s \mu_{ss})(\hat{p}_s - \hat{\pi}_s) \\ & + \frac{1}{2} \mu^{1/4} \left[\hat{p}_s \mu_{ss} \mu^{-(1/2)} \left(\hat{p}_s \mu^{1/4} \right) \right] + \frac{1}{2} \sum_k \hat{P}_k^2. \end{aligned} \tag{12}$$

The corresponding potential energy can be expanded in terms of Q_k. Here we stop at second order since the anharmonic terms are rarely available for large polyatomics; therefore,

$$\hat{V} = V_0(s) + \sum_k g_k(s) Q_k + \frac{1}{2} \sum_k \omega_k^2(s) Q_k^2, \tag{13}$$

with

$$g_k(s) = \sum_i \sum_\alpha (\partial V / \partial x_{i\alpha})_{x_{i\alpha} = a_{i\alpha}(s)} L_{i\alpha,k}(s) \tag{14}$$

and $\omega_k(s)$ is the frequency of mode k obtained by diagonalization of the projected Hessian matrix in the $3N$–7 small-amplitude degrees of freedom. As discussed by Tew *et al.* [6], although the geometry is optimized in internal (curvilinear) coordinates at each value of s, g_k does not vanish except at stationary points since the direction of motion along the path is not precisely parallel to the gradient, i.e. s and θ are not exactly the same.

The simplest approximation to $H = T + V$ is obtained by neglecting all the Coriolis couplings and the dependence of the $3N$–7 frequencies ω_k on s:

$$\begin{aligned} \hat{H}^{(0)} = {} & \frac{1}{2} \mu_{ss} \hat{p}_s^2 + \frac{1}{2} (\hat{p}_s \mu_{ss}) \hat{p}_s + \frac{1}{2} \mu^{1/4} \left[\hat{p}_s \mu_{ss} \mu^{-(1/2)} \left(\hat{p}_s \mu^{1/4} \right) \right] \\ & + V_0(s) + \frac{1}{2} \sum_k \left[\hat{P}_k^2(s_0) + \omega_k^2(s_0) Q_k^2 \right], \end{aligned} \tag{15}$$

where s_0 is the value of the internal coordinate corresponding to the most stable conformer of the molecule; i.e. V_0 has a global minimum at $s = s_0$. We take the separable Hamiltonian in equation (15) to be the zeroth-order Hamiltonian and solve the more exact Hamiltonian given by equations (12) and (13) approximately using perturbation theory. Therefore, a convenient choice of basis is given by the direct product

$$\Psi_{m,n_1,n_2,\ldots,n_{3N-7}}(s, Q_1, Q_2, \ldots, Q_{3N-7}) = \psi_m(s) \prod_{k=1}^{3N-7} \chi_{n_k}(Q_k), \tag{16}$$

where $\psi_m(s)$ is the mth eigenfunction of the large-amplitude motion, and $\chi_{nk}(Q_k)$is a harmonic oscillator eigenfunction at $s = s_0$ with a number n_k of quanta in oscillator k. The zero-order Hamiltonian in equation (15) can then be solved by direct diagonalization using many basis functions in the large-amplitude coordinate s; its solution is straightforward

$$E^{(0)}_{m,n_1,n_2,\ldots,n_{3N-7}} = E_m + \sum_{k=1}^{3N-7}\left(n_k + \frac{1}{2}\right)\hbar\omega_k(s_0) \tag{17}$$

where E_m is the mth eigenvalue of the large-amplitude motion operator (first four terms in equation (15)).

The first-order correction to the energy in equation (17) is the average value of $H - H^{(0)}$ over the unperturbed states. In the representation of the chosen basis, $H - H^{(0)}$ has the diagonal matrix elements

$$\begin{aligned}
&E^{(1)}_{m,n_1,n_2,\ldots,n_{3N-7}} \\
&= \left\langle \psi_m(s)\prod_{k=1}^{3N-7}\chi_{n_k}(Q_k)\middle|\hat{H} - \hat{H}^{(0)}\middle|\psi_m(s)\prod_{k=1}^{3N-7}\chi_{n_k}(Q_k)\right\rangle \\
&= \frac{\hbar^2}{2}\sum_{\alpha,\beta=1}^{4}\sum_{k,l=1}^{3N-7}\left\{\langle\psi_m(s)|\mu_{\alpha\beta}(s)B_{kl,\alpha}(s)B_{kl,\beta}(s)\right. \\
&\qquad\left.\left[\frac{\omega_l(s)}{\omega_k(s)}\left(n_k + \frac{1}{2}\right)\left(n_l + \frac{1}{2}\right) - \frac{1}{4}\right]|\psi_m(s)\rangle\right\} \\
&\quad + \hbar\sum_{k=1}^{3N-7}\langle\psi_m(s)|\omega_k(s) - \omega_k(s_0)|\psi_m(s)\rangle\left(n_k + \frac{1}{2}\right).
\end{aligned} \tag{18}$$

The off-diagonal blocks of the full Hamiltonian contain all of the coupling matrix elements involving different vibrational states. We take into account the corrections due to the large-amplitude motion coupling with the vibrational modes and the gradient of the potential using second-order perturbation theory

$$\begin{aligned}
&E^{(2)}_{m,n_1,n_2,\ldots,n_{3N-7}} = E^{\text{coriolis}(2)}_{m,n_1,n_2,\ldots,n_{3N-7}} + E^{\text{gradient}(2)}_{m,n_1,n_2,\ldots,n_{3N-7}} \\
&= \sum_{m',n'_1,n'_2,\ldots,n'_{3N-7}}\left\{\frac{\left|\left\langle\psi_m(s)\prod_{k=1}^{3N-7}\chi_{n_k}(Q_k)\right| - (1/2)\mu_{ss}(s)(\hat{p}_s\hat{\pi}_s + \hat{\pi}_s\hat{p}_s) - (1/2)[\hat{p}_s\mu_{ss}(s)]\hat{\pi}_s\left|\psi_{m'}(s)\prod_{l=1}^{3N-7}\chi_{n'_l}(Q_l)\right\rangle\right|^2}{E_{m,n_1,n_2,\ldots,n_{3N-7}} - E_{m',n'_1,n'_2,\ldots,n'_{3N-7}}}\right. \\
&\qquad\left. + \frac{\left|\left\langle\psi_m(s)\prod_{k=1}^{3N-7}\chi_{n_k}(Q_k)\right|\sum_k g_k(s)Q_k\left|\psi_{m'}(s)\prod_{l=1}^{3N-7}\chi_{n'_l}(Q_l)\right\rangle\right|^2}{E_{m,n_1,n_2,\ldots,n_{3N-7}} - E_{m',n'_1,n'_2,\ldots,n'_{3N-7}}}\right\} \\
&(m,n_1,n_2,\ldots,n_{3N-7}) \neq (m',n'_1,n'_2,\ldots,n'_{3N-7}) \\
&= \frac{\hbar^2}{16}\sum_{m'}\sum_{l>k}^{3N-7}\left(\left|\langle\psi_m(s)|\hat{H}^{\text{coriolis}(-)}_{k,l}|\psi_{m'}(s)\rangle\right|^2\left\{\frac{n_k n_l}{E_m - E_{m'} + \hbar[\omega_k(s_0) + \omega_l(s_0)]} + \frac{(n_k+1)(n_l+1)}{E_m - E_{m'} - \hbar[\omega_k(s_0) + \omega_l(s_0)]}\right\}\right. \\
&\quad\left. + \left|\langle\psi_m(s)|\hat{H}^{\text{coriolis}(+)}_{k,l}|\psi_{m'}(s)\rangle\right|^2\left\{\frac{(n_k+1)n_l}{E_m - E_{m'} - \hbar[\omega_k(s_0) - \omega_l(s_0)]} + \frac{n_k(n_l+1)}{E_m - E_{m'} + \hbar[\omega_k(s_0) - \omega_l(s_0)]}\right\}\right) \\
&\quad + \frac{\hbar}{2}\sum_{m'}\sum_{k=1}^{3N-7}\left|\langle\psi_m(s)|\omega_k^{-1/2}(s)g_k(s)|\psi_{m'}(s)\rangle\right|^2\left[\frac{n_k}{E_m - E_{m'} + \hbar\omega_k(s_0)} + \frac{n_k+1}{E_m - E_{m'} - \hbar\omega_k(s_0)}\right]
\end{aligned} \tag{19}$$

with

$$\begin{aligned}
&\langle\psi_m(s)|\hat{H}^{\text{coriolis}(\mp)}_{k,l}|\psi_{m'}(s)\rangle \\
&= \langle\psi_m(s)|\left\{\hat{p}_s\mu_{ss}(s)B_{kl,s}(s)\frac{\omega_l(s) \mp \omega_k(s)}{[\omega_k(s)\omega_l(s)]^{1/2}}\right. \\
&\qquad\left. + \mu_{ss}(s)B_{kl,s}(s)\frac{\omega_l(s) \mp \omega_k(s)}{[\omega_k(s)\omega_l(s)]^{1/2}}\hat{p}_s\right\}|\psi_{m'}(s)\rangle.
\end{aligned} \tag{20}$$

These perturbative expressions for the internal rotation–vibrational energy levels hold only in the absence of resonances. In this case, resonances occur when $E_m - E_{m'} \approx \pm\hbar[\omega_k(s_0) \pm \omega_l(s_0)]$ or $E_m - E_{m'} \approx \pm\hbar\omega_k(s_0)$. For this work, terms in equation (19) are removed if the numerator is greater than or equal to its corresponding denominator.

3. *Ab initio* calculations

Ab initio electronic structure calculations were carried out with the Gaussian 98 package [7] using the B3LYP hybrid density functional [9]. The basis set used was

the augmented triple zeta basis 6-311 + G(2df,2pd). For *ortho*-chlorotoluene, the torsional potential was calculated by constraining the dihedral angle at 10° increments relative to a local frame and optimizing all other internal coordinates to minimize the total energy. In the following paragraph we discuss the different possible definitions for the internal rotation angular coordinate. The geometry optimizations were carried out with the 'OPT = Tight' option, and the force constant matrix was output by setting internal options using the 'IOP(7/33 = 1)' keyword. Each resulting geometry was translated to the center of mass frame, and all Cartesian components as a function of s were fit to a Fourier series. In this way, finite differences can be used to numerically solve for the Euler angles which rotate the Cartesian axes and force constant matrix to align the molecule along an Eckart frame.

In general, there are several ways to parameterize any given large-amplitude torsion. Restricting consideration to a single dihedral angle is the conventional definition which is often used. However, a carefully chosen torsional coordinate θ must meet the requirement that the potential reaches the minimum at the same molecular configurations. For the specific case of chlorotoluene, the dihedral angle as shown in figure 1 does not fulfil this requirement. Furthermore, none of the dihedral angles between the CH_3 group and the benzene ring fulfils this requirement. As the torsional angle is changed, the C_{3V} point group symmetry of the CH_3 group is broken through the relaxation of the CH_2 bond angles. If one chooses to parameterize the entire torsional motion ($0 < \theta < 2\pi$) by a single dihedral internal coordinate, geometries at θ and $\theta + 2\pi/3$ do not correspond to the same molecular configuration (figure 2). Nevertheless, the Hamiltonian must be periodic with respect to symmetrically related molecular configurations. Any periodic path connecting the first-order saddle points at the top of the torsional barriers to the minima (the global equilibrium structures) on the potential energy surface will be accurately described by the internal coordinate path Hamiltonian. The true minimum energy path, however, is constructed such that the tangent at each point on the path points in the direction of the gradient. To make the gradient term $g_k(s)$ as small as possible, it is necessary to choose a path as close as possible to the minimum energy path. In the particular case of chlorotoluene, the true intrinsic reaction path coordinate more closely resembles (but still approximates) an average of all the dihedral angles between the CH_3 group and the benzene ring. In many cases, one can ensure the path s goes through the saddle points by taking advantage of molecular symmetry. At the equivalent minima and maxima, molecular symmetry is enforced by omitting the 'NOSYM' keyword; for all other geometries between the minimum and maximum, symmetry is completely disabled by including the 'NOSYM' keyword. Without this intervention, the constrained optimizations would not have located the symmetric saddle points and minima, and the potential $V_0(s)$ obtained would have lacked the true symmetry of the path. The resulting path using this method also satisfies the requirement that equal and opposite geometries from a symmetric point are assigned to mirror image configurations. The fully symmetric internal coordinate path, energies, and force constant matrices can thus be constructed from the information from one minimum to the next maximum using point group operations in a local frame (figure 3).

The frequencies and eigenvectors of the $3N$–7 orthogonal vibrational modes were obtained by diagonalizing the projected force constant matrix, where the s coordinate as well as the translations and rotations were projected out. For each value of the dihedral angle, the ordering of the frequencies and eigenvectors by diagonalization is arbitrary. However, this labelling does not correspond to the physical identity of the modes since modes of different symmetry may cross as a function of s. In order to obtain the correct ordering of frequencies and eigenvectors, we used a spline interpolation scheme to estimate the projected force constant matrix at several points between dihedral angle intervals. Dot products were then calculated between the eigenvectors at consecutive

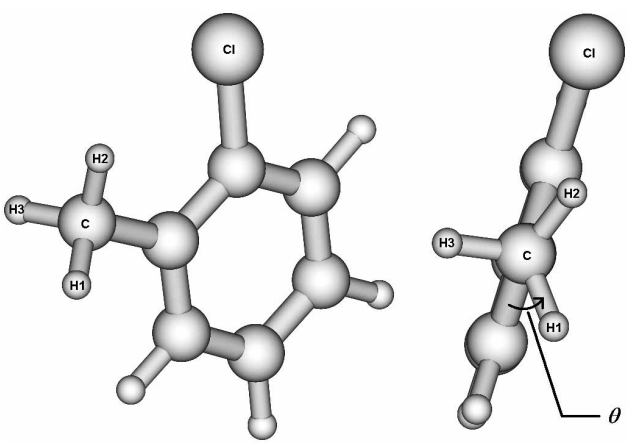

Figure 1. *Ortho*-chlorotoluene and internal coordinate θ.

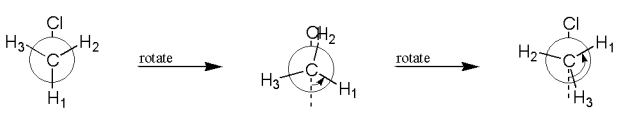

Figure 2. Exaggerated Newman projections of *ortho*-chlorotoluene indicating the torsional angle, which is defined as the dihedral angle between the H_1CC plane and the benzene ring plane. Freezing this coordinate in the geometry optimization does not result in symmetric H–Cl eclipsed conformations.

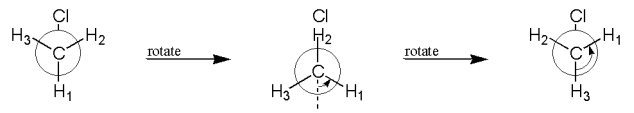

Figure 3. Newman projection of *ortho*-chlorotoluene with symmetric eclipsed structures obtained by enforcing symmetry when optimizing the stationary points. The true coordinate path is approximately a linear combination of all possible dihedral angles, but even this definition of s does not yield a path invariant to permutations of the H atoms.

points along s. Introducing factors of -1 and relabelling eigenvectors to maximize consecutive dot products generated a set of physically meaningful smoothly varying frequencies and orthogonal vibrational modes. Analytical forms for the energy $V_0(s)$ and the frequencies $\omega_k(s)$ along the internal coordinate path were obtained by fitting to linear combinations of sine and cosine functions.

We should also mention that the B3LYP 6-31G(d,p) method (which was not used for any of the calculations reported here) is qualitatively but not quantitatively accurate for the case studied. In particular, it provided a correct model for ordering and crossing of frequencies, but failed in our hands to give smoothly varying eigenvectors, which are essential to evaluating coupling elements between normal modes and the large-amplitude coordinate. We recommend using a large basis for accurately calculating the orthogonal vibrational modes and their coupling elements.

4. *Ortho*-chlorotoluene

A complete geometry optimization of *ortho*-chlorotoluene finds the minimum energy to be of Cs symmetry with $\theta = 0$ (figure 1). The barrier to internal rotation was $402\,\mathrm{cm}^{-1}$ with B3LYP/6-311 + G(2df,2pd). The barrier in *ortho*-chlorotoluene has not been experimentally determined, but microwave measurements place a lower limit of $400\,\mathrm{cm}^{-1}$ on its value [10]. Figure 4 shows the variation of the harmonic frequencies as a function of the internal coordinate path, which indicates a mixing of the torsion with other vibrational modes. The torsional potential in *ortho*-chlorotoluene possesses three equivalent minima as the molecule contains three equilibrium configurations along the torsional coordinate.

We obtained the $J = 0$ partition function for *ortho*-chlorotoluene by numerical summation over all internal rotation–vibrational energy levels and their first- and second-order perturbations

$$Q = \sum_j e^{-E_j/k_B T}. \tag{21}$$

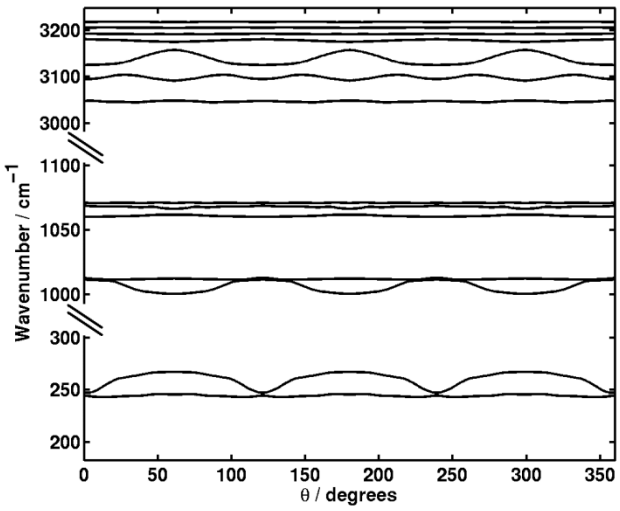

Figure 4. Harmonic wavenumbers of *ortho*-chlorotoluene as a function of the internal coordinate θ. The derivatives $L'(s)$ and therefore the terms $B_{kl}(s)$ in the Hamiltonian can fluctuate rapidly at geometries where vibrational frequencies become nearly degenerate, leading to large couplings between the small-amplitude and large-amplitude coordinates.

The partition function in this paper is defined with the zero of energy at the lowest quantum state; i.e. the partition function is bounded from below by unity. We retain only those energies with $E_j < \varepsilon$ where ε is an energy cutoff parameter so that the error due to the limited number of states included in the partition function is negligible for the temperature of interest. We chose $\varepsilon = 3170\,\mathrm{cm}^{-1}$ so that the error in the summation of the 1.3×10^6 energy levels is insignificant for temperatures less than 300 K. To check the validity of the Pitzer–Gwinn method, we compare results obtained from equation (21) with the conventional $J = 0$ partition function Q_{PGHO} obtained by a product of partition functions associated with internal rotational and vibrational motions

$$Q_{\mathrm{PGHO}} = Q_{\mathrm{HR}} \prod_{k=1}^{3N-7} Q_{\mathrm{vib},k}. \tag{22}$$

$Q_{\mathrm{vib},k}$ is the conventional partition function for the kth vibrational mode

$$Q_{\mathrm{vib},k} = \frac{1}{1 - \exp\left[-\hbar\omega_k(s_0)/k_B T\right]}. \tag{23}$$

Q_{HR} is the hindered rotor partition function obtained by summation over energy levels for the effective Schrödinger equation

$$-\frac{\hbar^2}{2I_r}\frac{d^2\Psi(\phi)}{d\phi^2} + V(\phi)\Psi(\phi) = E\Psi(\phi), \tag{24}$$

where I_r is the reduced moment of inertia of the two rotating groups about an axis passing through the center of gravity of both the groups. In the notation of East and Radom [11], this method of calculating the reduced moment of inertia is the $(m,n) = (2,3)$ representation. The reduced moment of inertia for *ortho*-chlorotoluene was 2.99 amu Å^2 using the most stable molecular conformer at $s = s_0$.

Figure 5 shows the percent deviation of the partition function Q from Q_{PGHO} calculated at various levels of approximation. This figure compares the deviation by neglecting certain perturbative corrections to the zeroth-order energy used to calculate Q. For these comparisons, the following labeling scheme was used: Q calculated from all first- and second-order perturbations is labelled FULL; Q calculated by including only the first-order perturbation due to $\omega_k(s) - \omega_k(s_0)$ is labelled POT-1; Q calculated by including only the first-order perturbation due to the term proportional to $\mu_{\alpha\beta} B_{kl,\alpha} B_{kl,\beta}$ is labelled G-1; Q calculated by including only the second-order perturbation due to $g_k(s) Q_{\ k}(s)$ is labelled GRAD-2; Q calculated by including only the second-order perturbation due to $-1/2\mu_{ss}(p_s\pi_s + \pi_s p_s) - 1/2(p_s\mu_{ss})\pi_s$ is labelled COR-2. The results from the Pitzer–Gwinn partition function are within 1% of the partition function Q calculated at any level of approximation for temperatures less than 60 K. All other deviations from Q behave quite differently at higher temperatures for the case studied. Figure 5 shows most of the deviation from the Pitzer–Gwinn trend is attributed to the first-order term G-1 and the second-order term COR-2. However, the separate contributions due to G-1 and COR-2 tend to cancel each other at higher temperatures; as a result, the full calculation is within a fraction of a percent of the Pitzer–Gwinn approximation. The other perturbative terms POT-1 and GRAD-2 both deviate from the Pitzer–Gwinn partition function by less than 2%. We should mention that special care must be taken in the calculation of terms containing the Coriolis couplings such as $\mu_{\alpha\beta} B_{kl,\alpha} B_{kl,\beta}$ and $-1/2\mu_{ss}(p_s\pi_s + \pi_s p_s) - 1/2(p_s\mu_{ss})\pi_s$ if the ordering of harmonic frequencies $\omega_k(s)$ change as a function of s. The avoided crossings of harmonic frequencies are usually accompanied by large couplings between the small-amplitude vibrations and the large-amplitude motion. These large couplings can be sharply peaked in the vicinity of avoided crossings. This is particularly true for large molecules with their dense spectra of harmonic frequencies such as *ortho*-chlorotoluene (figure 4). In view of the fact that these couplings may be highly exaggerated due to the particular *ab initio* calculation used, it may be reasonable to eliminate these couplings if they are greater than a cutoff value. We did not examine this and included all the couplings in our calculations.

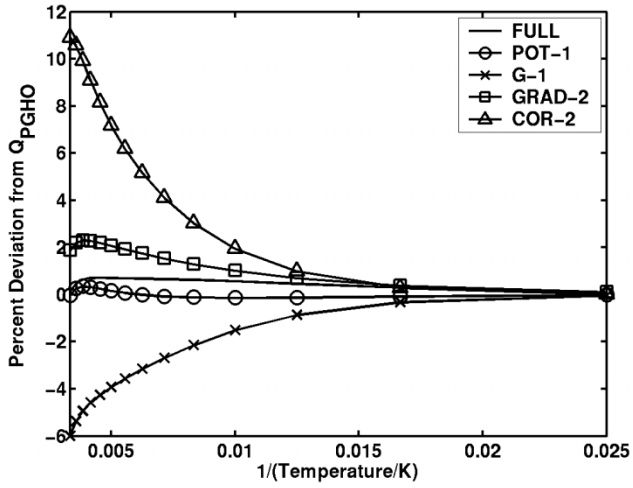

Figure 5. Deviations between the Pitzer–Gwinn partition function and partition functions computed here for *ortho*-chlorotoluene. For this molecule, the full calculation including all first- and second-order perturbations deviates by a few per cent from the conventional partition function.

5. Conclusions

Here we have developed a perturbation theory treatment of the important situation where one large-amplitude motion is coupled to a set of small-amplitude motions based on the Hamiltonian developed by Handy and co-workers [6]. Our perturbation theory treatment, which requires only a few dozen geometry optimizations and second-derivative calculations, is expected to be more practical for routine partition function calculations on large polyatomics and transition states than the more exact variational approach used in Carter, Handy, and Bowman's MULTIMODE program [12, 13, 14]. Here we have applied the perturbative approach to study *ortho*-chlorotoluene, as a typical example of a large (39 vibrational modes) molecule with a methyl rotor, and we have compared our results with the conventional Pitzer–Gwinn approach. The perturbative approach makes it easy to identify which coupling terms are most important for accurately computing the partition function and which terms contribute most to the difference between this approach and the conventional Pitzer–Gwinn model. We have also presented a method for forcing the zeroth-order Hamiltonian to maintain the permutation symmetry of the true Hamiltonian; most methods for constructing the large-amplitude path do not preserve this symmetry.

To our knowledge, this is the first test in the literature of the crucial separability assumption of the

Pitzer–Gwinn approximation for a large polyatomic molecule. In this case (a symmetric methyl rotor attached to a much heavier group), the separability assumption corresponds to a small (<10%) error in the $J = 0$ partition function. The previously untested but widely used Pitzer approximations are quite accurate for methyl rotors! Future research will focus on heavier asymmetric top rotors, where one might expect the Pitzer approximations to be less accurate, and the neglected couplings with the external rotations will be more important.

Acknowledgements

Preliminary work by Dr Oleg Mazyar and interesting conversations with Dr Stuart Carter are gratefully acknowledged. This work was supported by the Office of Basic Energy Sciences, Offices of Energy Research, US Department of Energy under Grant No. DE-FG02-98ER14914.

References

[1] H.S. Johnston, *Gas Phase Reaction Rate Theory*, Ronald Press, New York (1966).
[2] K.S. Pitzer, W.D. Gwinn, *J. Chem. Phys.*, **10,** 428 (1942).
[3] K.S. Pitzer, *J. Chem. Phys.*, **14,** 239 (1946).
[4] D. Papoušek, M.R. Aliev, *Molecular Vibrational-Rotational Spectra*, Elsevier Scientific Publishing Company, New York (1982).
[5] http://webbook.nist.gov/chemistry/ (accessed 11 August 2004)
[6] T.P. Tew, N.C. Handy, S. Carter, S. Irle, J. Bowman, *Mol. Phys.*, **101,** 3513 (2003).
[7] M.J. Frisch, G.W. Trucks, H.B. Schlegel, G.E. Scuseria, M.A. Robb, J.R. Cheeseman, V.G. Zakrzewski, J.A. Montgomery, R.E. Stratmann, J.C. Burant, S. Dapprich, J.M. Millam, A.D. Daniels, K.N. Kudin, M.C. Strain, O. Farkas, J. Tomasi, V. Barone, M. Cossi, R. Cammi, B. Mennucci, C. Pomelli, C. Adamo, S. Clifford, J. Ochterski, G.A. Petersson, P.Y. Ayala, Q. Cui, K. Morokuma, D.K. Malick, A.D. Rabuck, K. Raghavachari, J.B. Foresman, J. Cioslowski, J.V. Ortiz, A.G. Baboul, B.B. Stefanov, G. Liu, A. Liashenko, P. Piskorz, I. Komaromi, R. Gomperts, A.L. Martin, D.J. Fox, T. Keith, M.A. Al-Laham, C.Y. Peng, A. Nanayakkara, M. Challacombe, P.M.W. Gill, B. Johnson, W. Chen, M.W. Wong, J.L. Andres, C. Gonzalez, M. Head-Gordon, E.S. Replogle, J.A. Pople, Gaussian 98, revision A.11.4, Gaussian, Inc., Pittsbugh, PA (1998).
[8] S. Carter, N.C. Handy, *J. Chem. Phys.*, **113,** 987 (2000).
[9] (a) A.D. Becke, *Phys. Rev.* A, **38,** 3098 (1988); (b) C. Lee, W. Yang, R.G. Parr, *Phys. Rev.* B, **37,** 785 (1988); (c) A.D. Becke, *J. Chem. Phys.*, **98,** 5648 (1993).
[10] K.P.R. Nair, K. Epple, *Chem. Phys. Lett.*, **166,** 146 (1990).
[11] A.L.L. East, L. Radom, *J. Chem. Phys.*, **106,** 6655 (1997).
[12] S. Carter, J.M. Bowman, L.B. Harding, *Spectrochim. Acta* A, **53,** 1179 (1997).
[13] S. Carter, S. Culik, J.M. Bowman, *J. Chem. Phys.*, **107,** 10458 (1997).
[14] S. Carter, J.M. Bowman, N.C. Handy, *Theor. Chem. Acc.*, **100,** 191 (1998).